

Comparison between Graphene and GaAs Quantized Hall Devices with a Dual Probe

Shamith U. Payagala, Albert F. Rigosi, Alireza R. Panna, Alessio Pollarolo, Mattias Kruskopf, Stephan Schlamminger, *Member, IEEE*, Dean G. Jarrett, *Senior Member, IEEE*, Ryan Brown, Randolph E. Elmquist, *Senior Member, IEEE*, Duane Brown, David B. Newell*

Abstract— A graphene quantized Hall resistance (QHR) device fabricated at the National Institute of Standards and Technology (NIST) was measured alongside a GaAs QHR device fabricated by the National Research Council of Canada (NRC) by comparing them to a 1 k Ω standard resistor using a cryogenic current comparator. The two devices were mounted in a custom developed dual probe that was then assessed for its viability as a suitable apparatus for precision measurements. The charge carrier density of the graphene device exhibited controllable tunability when annealed after Cr(CO)₃ functionalization. These initial measurement results suggest that making resistance comparisons is possible with a single probe wired for two types of quantum standards – GaAs, the established material, and graphene, the newer material that may promote the development of more user-friendly equipment.

Index Terms— dual probe assembly, quantized Hall resistance, epitaxial graphene, cryogenic current comparator, carrier density

I. INTRODUCTION

THE implementation of graphene-based quantized Hall resistance (QHR) standards over the recent years has simplified the efforts needed to realize the ohm at National Metrology Institutes (NMIs) and primary standards laboratories [1] – [9]. To make standards easier to use, it is crucial that graphene devices are prepared such that their electrical properties, most prominently the charge carrier density (n), can be controllably tuned. In the past, graphene devices at the National Institute of Standards and Technology (NIST) have been stored in an argon environment to assist in stabilizing n . Regardless of this environment, the long-term stability of graphene QHR devices in ambient laboratory conditions remained an issue.

Manuscript received March 17, 2020; revised April 10, 2020. **The first three authors contributed equally to this manuscript.** For a subset of the author list, this work was prepared as part of their official duties for the U. S. Government. *Asterisk indicates corresponding author.*

S. U. Payagala, A. F. Rigosi, A. R. Panna, S. Schlamminger, D. G. Jarrett, R. E. Elmquist, and D. B. Newell are with the National Institute of Standards and Technology, Gaithersburg, MD 20899, USA (corresponding author e-mail: david.newell@nist.gov).

M. Kruskopf is with the Physikalisch-Technische Bundesanstalt, Braunschweig 38116, Germany

A. Pollarolo, R. Brown, and D. Brown are with Measurements International, Ltd., Prescott, Ontario, K0E 1T0, Canada

In the past year, techniques for preparing graphene devices for long term storage and functionality have been increasing in popularity [10] – [13]. Because of the device preparation methods contained herein, the shelf-life of these devices has increased to years [10] – [11], making them a viable and robust option for performing international comparisons.

To continue the transition to using new graphene-compatible technologies, a dual probe system was designed and tailored specifically for comparisons utilizing two QHR devices in a cryostat that does not require the purchase or handling of liquid cryogenes. Such a system holds numerous advantages over others, including the removal of laboratory hazards associated with handling liquid cryogenes, as well as a reduction in the financial burden imposed by periodic replenishment. Furthermore, the use of a dual probe allows end users to self-verify full functionality of their QHR devices by enabling comparisons to be done with both devices simultaneously. Though the literature includes some work on dual probes [14] – [15], demonstrations of international comparisons on this kind of measurement system are lacking, with some systems needing multiple cryostats [2, 4, 6], liquid cryogen replenishment [1, 5, 6, 14], or even more expensive cryogen mixtures (i.e. ³He) to reach temperatures below 1 K [2, 3, 4, 14].

For this system, a GaAs QHR device was provided by the National Research Council of Canada (NRC) and NIST provided the graphene QHR device. In addition to the dual probe and its cryostat, a cryogenic current comparator (CCC) bridge was used to assess the quality of the QHR devices. The transition to using graphene-based devices would promote the development of more user-friendly equipment because of graphene’s larger parameter space of functionality. Furthermore, dual probe functionality enables the addition of future QHR array devices that output different quantized resistances [16] – [22]. This enhancement would lead to a measurement system having two distinct starting points in a calibration chain as opposed to the usual single value (12.9 k Ω), thus shortening the calibration chain, allowing for simultaneous comparisons, and reducing the need for additional cryostats. A dual- or multiple-device probe would also facilitate realization of the main ratio arms of a quantum Wheatstone bridge [23, 24].

II. SAMPLE PREPARATION

Wafers of GaAs were grown using molecular beam epitaxy by the Institute for Microstructural Sciences at NRC. Devices were fabricated using standard ultraviolet photolithography and wet etching techniques. Deposited and annealed multi-layer AuGeNi films were used as electrical contacts. The device was mounted onto a transistor outline (TO-8) package. An example magnetic flux density sweep is shown in Fig. 1 (a), along with an optical image of the device.

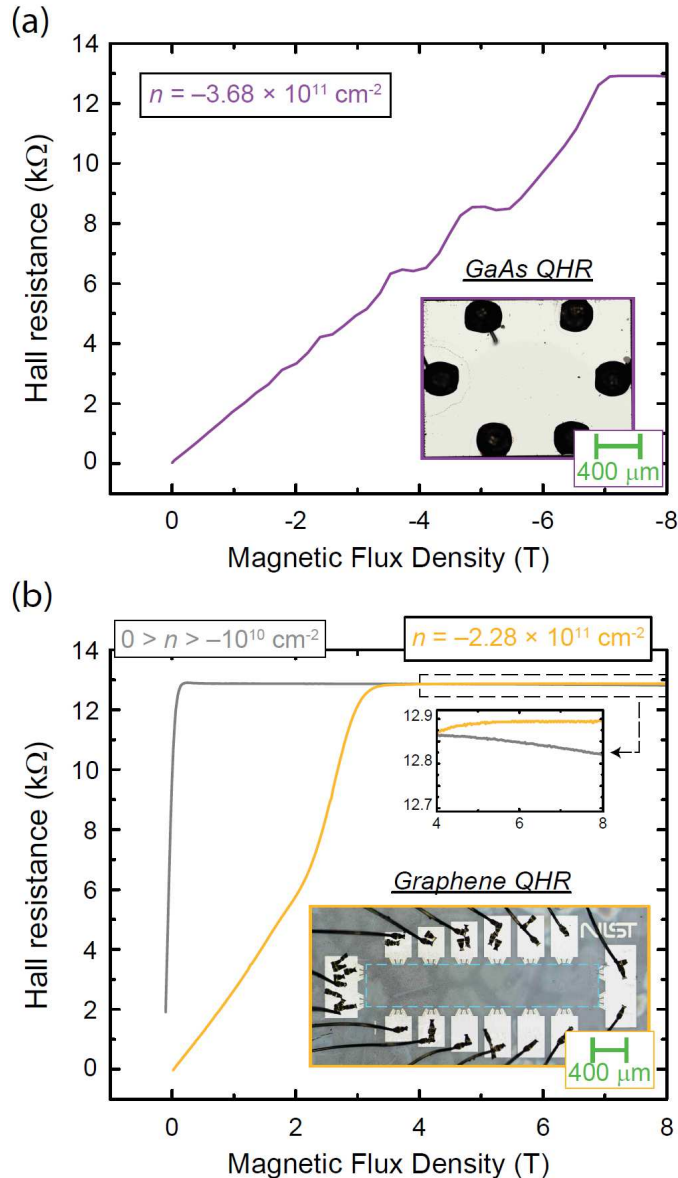


Fig. 1. (a) An example magnetoresistance measurement is shown for the GaAs-based QHR device. The inset contains an optical image of the actual device (n -type). The calculated charge carrier density is determined by the linear behavior near 0 T. (b) Two example magnetoresistance measurements are shown for the graphene-based QHR device. The gray curve represents an unannealed device after functionalization. A scale magnification reveals that the Hall resistance is not well-quantized, thus requiring an annealing process. The gold curve represents the device after annealing for approximately 20 min at 350 K. The inset contains an optical image of the actual device (n -type).

Graphene is epitaxially grown on the Si-face of silicon carbide (SiC) by sublimating Si atoms from the substrate at

high temperatures. The surface then becomes enriched with carbon atoms that reconstruct as a honeycomb lattice. SiC substrates were diced from on-axis 4H-SiC(0001) semi-insulating wafers. The growth was performed using both the face-to-graphite orientation on a disk of glassy carbon and polymer-assisted-sublimation growth (PASG) [25]. All graphene devices were processed in the same resistive-element furnace with heating and cooling rates of approximately 1.5 K/s. The graphite-lined chamber provided a homogeneous background temperature and was flushed with argon gas prior to the final fill of 100 kPa argon from a 99.999 % liquid argon source. Temperatures were increased to a maximum of 1900 °C for about 270 s annealing time in an argon atmosphere.

Finished graphene substrates were prepared by methods already documented in the literature, [26] – [27]. To summarize the fabrication process, graphene is protected by a layer of Pd-Au to prevent organic contamination. Photolithography is then used to obtain a Hall bar geometry and electrical contacts. Notable differences between this method and previous work are primarily in the layout of the electrical contacts. The orthogonal contact pairs seen in Fig. 1 (b) have varying lateral dimensions and are symmetric with respect to the length of the device. These differences were implemented in the hope of assessing any measurable relationship between the contact shape and its corresponding resistance. The graphene device is then functionalized with $\text{Cr}(\text{CO})_3$, as described in [11], and mounted onto a leadless chip carrier with 32 pins (LCC-32).

Contact resistances were measured at 9 T and approximately 2 K by using a three-terminal configuration, whereby a source is placed on an arbitrary contact and a drain is placed on the contact of interest. Two voltage leads are then placed on two additional contacts – the drain contact and another contact along the same equipotential line (in the quantum Hall regime). These measurements yielded contact resistances on the order of 0.1 Ω, with the exception of two contacts that measured less than 5 Ω, perhaps due to a fabrication defect. There were no reproducible patterns between the contact resistances and the different contact pad dimensions.

Fig. 1 (b) shows a positive magnetic flux density measurement of the Hall resistance, which exhibits only the $\nu = 2$ plateau ($R_K/2 \approx 12.9 \text{ k}\Omega$). There are two curves shown. The gray curve is the corresponding sweep for an unannealed device after functionalization with $\text{Cr}(\text{CO})_3$. Though this plateau appears flat, a scale magnification reveals that the Hall resistance is not well-quantized, primarily due to the mixture of electron and hole puddles that form with n close to the Dirac point of graphene. The gold curve shows the same device after annealing at 350 K for approximately 20 min. It should be noted that this annealing process is required anytime the device is kept in air for more than one day, after which the device maintains a low carrier density ($< 10^{10} \text{ cm}^{-2}$) for periods on the order of years [6]. The annealing process reproducibly yields a similar n each time it is performed, as per the analysis done on the metric known as the integrated heat exposure [11].

III. MEASUREMENT SYSTEM

The primary measurement system comprises the cryostat, dual probe assembly, CCC, and 1 k Ω standard resistor. The cryostat was assembled with a helium recovery system and only required gaseous helium for operation (with room temperature gas being cooled to liquid temperatures). It was fitted with a 9 T superconducting magnet (with field homogeneity within 0.1 % per cm in the plane of the sample) and reached a base temperature of 1.18 K, which was not steadily controllable. All measurements were made at this lowest temperature. The dual probe assembly was constructed to accommodate both GaAs-based and graphene-based QHR devices. The challenge of this construction lies mostly with the possible introduction of leakage paths to ground, thermal strain on cooling power near the sample, and electrical noise. An image of the sample holder is shown in Fig. 2. One should note that the magnetic field directions experienced by both devices are of opposite sign due to the design of the sample holder.

A CCC resistance bridge was equipped with digital current sources [28], a low-noise voltmeter based on a chopper amplifier [29], and a DC superconducting quantum interference device (SQUID). Currents of 38.7 μ A (0.5 V) and 77.5 μ A (1 V) were used for all measurement configurations.

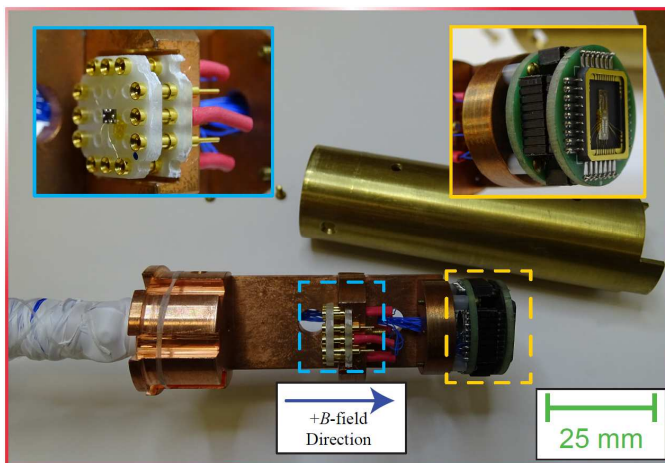


Fig. 2. An image of the sample holder on the dual probe assembly is shown. It accommodates both TO-8 and LCC-32 chip packages. To have all wires share an exit point, the sample holder was designed such that the devices experience magnetic fields with opposite sign.

The 1 k Ω standard resistor was calibrated using the CCC at 38.7 μ A (0.5 V). A subset of historical data is shown in Fig. 3 and a linear regression was used to predict the present-day value of the resistor (blue curve and left vertical axis), with secondary support from a calculation of the residuals (red curve and right vertical axis). This prediction was the basis on which the QHR devices in the dual-probe system were compared.

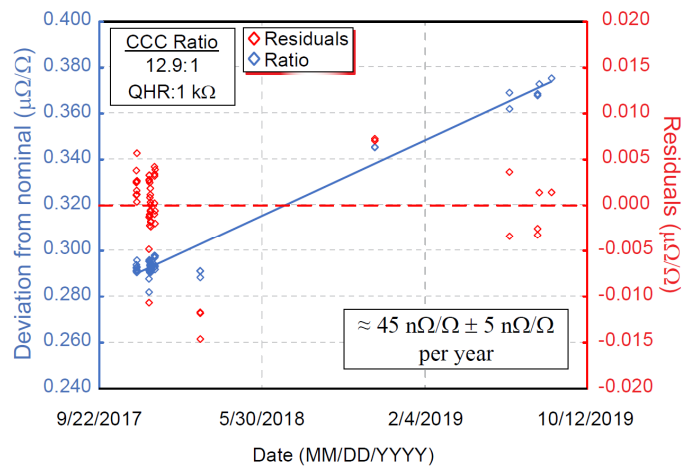


Fig. 3. CCC-acquired calibration data for the standard resistor are shown over the course of several years and provide a stable basis for estimating the present-day value of the resistor. Blue is used for the left vertical axis to represent the deviation from the nominal resistor value. Data were taken at 38.7 μ A (0.5 V). All information pertaining to the residuals are colored in red and are coupled to the right vertical axis. Error bars indicating Type A uncertainty are smaller than the data points.

IV. RESULTS FROM QHR DEVICES

The predicted value of the 1 k Ω resistor, based on a prior history of CCC measurements, drifted over the course of a few days by less than 1 n Ω/Ω , which was too small to detect with our measurements. Both QHR device measurements were performed in close succession (within a few days) to obtain data that correspond to approximately the same standard resistor value. Four varieties of CCC measurements were performed: Hall resistance of a left and right orthogonal pair and two corresponding diagonal measurements to assess the longitudinal resistivity (ρ_{xx}), which, in two dimensions, is related to the ratio of the two lateral dimensions of the region over which a resistance is measured. These Hall measurements are illustrated in Fig. 4 (a) and (b) for GaAs and graphene, respectively. All measurements were performed at the same magnetic flux density (+7.7 T).

The quality of device quantization comes from the conditions set forth by pertinent literature for DC quantum Hall measurements [30] – [31]. The critical currents for the QHR devices are approximately 100 μ A, since a criterion violation is present in the correction factor to the Hall resistivity, as defined by Ref. [31] (that such a correction factor should not exceed a few parts in 10^8). When measurements were performed at 116 μ A (1.5 V), the longitudinal resistivity was an order of magnitude larger, causing the above violation. For this reason, all comparisons were performed at 38.7 μ A (0.5 V) and 77.5 μ A (1 V).

A. Comparing GaAs Against the 1 k Ω Resistor

All GaAs QHR measurements were performed at the same field (+7.7 T), as per the condition observed in the magnetoresistance measurement in Fig. 1 (a). In Fig. 4 (c) a summary of both GaAs QHR measurements on two orthogonal Hall pairs are shown (recall that the NIST GaAs was used for calibrating the 1 k Ω standard resistor). For all

presented weighted mean data, the error bars indicate the Type A uncertainty at 1σ .

The differences between diagonal and orthogonal measurements made for a rectangular sample region gives the longitudinal resistances, and when multiplied by the ratio of the width to length (approximately 1.4:1), we find both resistivities to be about $(91.2 \pm 91.6) \mu\Omega$ at $38.7 \mu\text{A}$ (0.5 V) and $(173 \pm 55) \mu\Omega$ at $77.5 \mu\text{A}$ (1 V). Though higher than values seen in the literature, the CCC measurements still agree with those taken with the NIST GaAs, to within their Type A uncertainty, demonstrating that such agreements can be made with this measurement system.

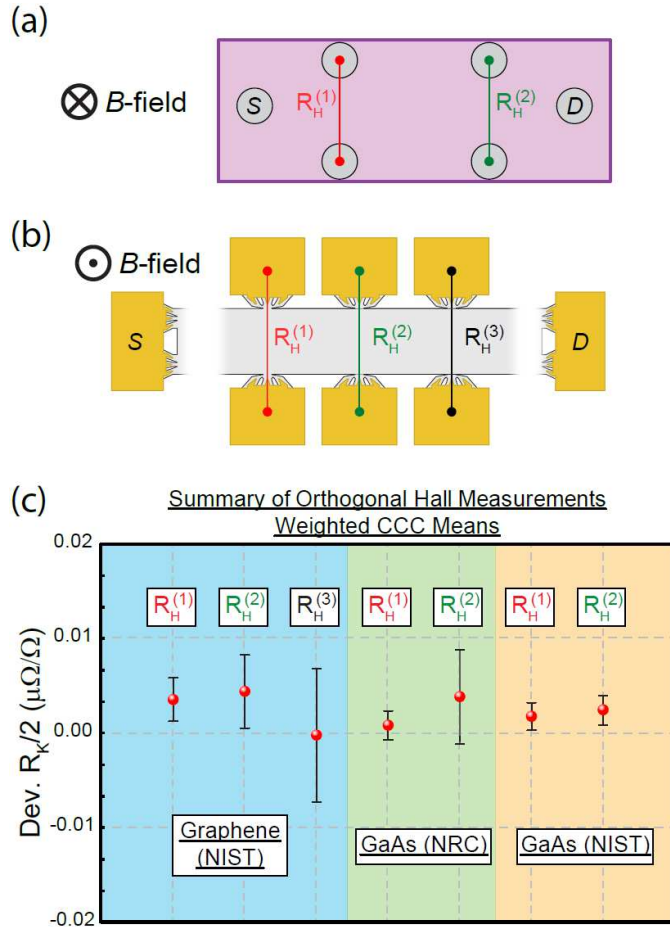


Fig. 4. (a) Illustration of the orthogonal measurements taken on the GaAs QHR and (b) graphene QHR device. (c) Weighted means of the CCC-obtained deviations from $R_k/2$ are shown; with the blue, green, and gold shading indicating the data for orthogonal pairs using NIST graphene, NRC GaAs, and NIST GaAs. The error bars represent Type A uncertainties at 1σ . All orthogonal pair data were collected at $38.7 \mu\text{A}$ (0.5 V) and $77.5 \mu\text{A}$ (1 V), with the exception of $R_H^{(3)}$, which was collected at the former.

B. Comparing Graphene Against the 1 k Ω Resistor

For the graphene measurements, the magnetic flux density was selected to match that of the GaAs QHR device. The same four measurements were performed with the CCC (Fig. 4 (b), which is not to scale). The three orthogonal pairs exhibited offsets from the predicted value not exceeding $5 \text{ n}\Omega/\Omega$. The first orthogonal pair had the smallest uncertainty of the set. All

Type A uncertainties (at 1σ), indicated by the error bars, of these weighted means are less than $10 \text{ n}\Omega/\Omega$. For the graphene QHR data, three sets of orthogonal pairs were measured, with the third pair measured only at 0.5 V and excluded from Table I to keep the comparison between both GaAs and the graphene devices consistent (two pairs each).

In a similar fashion, the longitudinal resistivity can be calculated for the two sides of the device, giving an assessment of the quantization. The width to length ratio is slightly smaller than that of GaAs (1.25:1). Taking the difference between the diagonal and orthogonal measurements, the longitudinal resistivities were found to be about $(229 \pm 154) \mu\Omega$ at $38.7 \mu\text{A}$ (0.5 V) and $(254 \pm 72.2) \mu\Omega$ at $77.5 \mu\text{A}$ (1 V). These values are also higher than values seen in the literature, and further discussion on the matter may be found below. It should be noted that only $R_H^{(1)}$ and $R_H^{(2)}$ were used for the uncertainty analysis.

C. Uncertainty Budget - Relative Deviation from $R_k/2$

The variation in Type A uncertainties seen in Fig. 4 (c) is most likely partially attributable to a non-ideal variation in local building ground and exhibited an unpredictable time-dependence. Additional attributions can be made to the manufactured cryostat, seeing as it did not have an isolator installed for the high-pressure gas lines connecting the system to the motorized compressor unit. Though the unit is housed in a separate area for vibration isolation and power line isolation, this lack of isolation introduces a second ground with interference from other mechanical motors. The electrical noise is higher in this case than when operating the CCC in a quiet laboratory power environment. Vibration in the measurement leads are also a source of noise and the grounding issue may interact with each lead to a different extent. Since increased noise and offsets have also been observed in different measurement setups when using a room-temperature direct current comparator (as a troubleshooting device), the noise problem is not likely to be an issue of SQUID noise rectification.

All relevant uncertainties have been summarized below in Table I. The dispersion of the bridge ratio readings were calculated separately for each device corresponding to the weighted mean of the deviation from nominal value. The combined standard uncertainty in each case reflects the uncertainty for the weighted means of the Hall resistivities measured at $77.5 \mu\text{A}$ (1 V) and $38.7 \mu\text{A}$ (0.5 V) for both graphene and GaAs. The leakage or insulation resistance was estimated to be $1 \text{ T}\Omega$. The CCC error was calculated as a residual sum of squares (RSS) that included the following four elements: (1) A ratio error that was measured using a build-up method, (2) The drift of the compensation network, (3) Any detector nonlinearity and gain errors, (4) Any errors due to noise rectification of the SQUID.

TABLE I
UNCERTAINTY BUDGET – RELATIVE DEVIATION FROM $R_K/2$

Parameter	Type	$u_i (k=1)$ ($n\Omega/\Omega$)
Dispersion of CCC Bridge Readings (NRC GaAs)	A	1.4
Dispersion of CCC Bridge Readings (NIST Graphene)	A	1.8
Leakage	B	1.0
CCC Electronics	B	3.0
Imperfect Quantization (NRC GaAs)	B	13.4
Imperfect Quantization (NIST Graphene)	B	18.7
Calibration of Standard Resistor	B	5.0
Combined (NRC GaAs)	RSS	14.7
Combined (NIST Graphene)	RSS	19.7

V. CONCLUSION

The CCC measurements presented herein yielded results suggesting that a dual probe (and its cryostat that does not require the handling of liquid cryogenics) can be used for low uncertainty measurements of graphene and show that the use of the latter provides expanded utility to multiple QHR devices quantized within a few parts in 10^8 . The improvement of these measurement systems should encourage the transition from using GaAs-based devices to using graphene-based devices. Doing so would promote the further development of more user-friendly equipment tailored to graphene's more relaxed parameter space of functionality.

ACKNOWLEDGMENT

The authors would like to thank Chieh-I Liu and Antonio Levy for their assistance in the NIST internal review process. The authors also thank the National Research Council of Canada for providing a GaAs QHR standard and the individuals involved with the establishment of the Cooperative Research and Development Agreement that made this work possible.

REFERENCES

- [1] Ribeiro-Palau R, Lafont F, Brun-Picard J, Kazazis D, Michon A, Cheynis F, Couturaud O, Consejo C, Jouault B, Poirier W, Schöpfer F. Quantum Hall resistance standard in graphene devices under relaxed experimental conditions. *Nature nanotechnology*. 2015 Nov;10(11):965.
- [2] Janssen TJ, Williams JM, Fletcher NE, Goebel R, Tzalenchuk A, Yakimova R, Lara-Avila S, Kubatkin S, Fal'ko VI. Precision comparison of the quantum Hall effect in graphene and gallium arsenide. *Metrologia*. 2012 Mar 29;49(3):294.
- [3] Tzalenchuk A, Lara-Avila S, Kalaboukhov A, Paolillo S, Syväjärvi M, Yakimova R, Kazakova O, Janssen TJ, Fal'ko V, Kubatkin S. Towards a quantum resistance standard based on epitaxial graphene. *Nature nanotechnology*. 2010 Mar;5(3):186.
- [4] Woszczyna M, Friedemann M, Götz M, Pesel E, Pierz K, Weimann T, Ahlers FJ. Precision quantization of Hall resistance in transferred graphene. *Applied Physics Letters*. 2012 Apr 16;100(16):164106.
- [5] Kučera J, Svoboda P, Pierz K. AC and DC quantum Hall measurements in GaAs-based devices at temperatures up to 4.2 K. *IEEE Transactions on Instrumentation and Measurement*. 2018 Dec 13;68(6):2106-12.
- [6] Bergsten T, Eklund G. Comparison between GaAs and graphene QHR standards for resistance realisation at SP. *Conference on Precision Electromagnetic Measurements (CPEM 2016)* 2016 Jul 10 (pp. 1-2). IEEE.
- [7] A. F. Rigosi, A. R. Panna, S. U. Payagala, M. Kruskopf, M. E. Kraft, G. R. Jones, B.-Y. Wu, H.-Y. Lee, Y. Yang, J. Hu, D. G. Jarrett, D. B. Newell, and R. E. Elmquist. Graphene Devices for Table-Top and High Current Quantized Hall Resistance Standards. *IEEE Trans. Instrum. Meas.* 68, 1870-1878, 2019.
- [8] T. J. B. M. Janssen, S. Rozhko, I. Antonov, A. Tzalenchuk, J. M. Williams, Z. Melhem, H. He, S. Lara-Avila, S. Kubatkin, and R. Yakimova, Operation of a Graphene quantum Hall resistance standard in cryogen-free table-top system, *2D Mater.*, 2, 035015, 1 – 9, 2015.
- [9] A. F. Rigosi and R. E. Elmquist. The Quantum Hall Effect in the Era of the New SI. *Semicond. Sci. Technol.* 34, 093004 (2019).
- [10] He H, Lara-Avila S, Kim KH, Fletcher N, Rozhko S, Bergsten T, Eklund G, Cedergren K, Yakimova R, Park YW, Tzalenchuk A. Polymer-encapsulated molecular doped epigraphene for quantum resistance metrology. *Metrologia*. 56, 045004, 2019.
- [11] A. F. Rigosi, M. Kruskopf, H. M. Hill, H. Jin, B. Y. Wu, *et al.* Gateless and reversible Carrier density tunability in epitaxial graphene devices functionalized with chromium tricarbonyl. *Carbon*, 142, 468–474, 2019.
- [12] He, H., Kim, K.H., Danilov, A., Montemurro, D., Yu, L., Park, Y.W., Lombardi, F., Bauch, T., Moth-Poulsen, K., Iakimov, T. Yakimova, R. Uniform doping of graphene close to the Dirac point by polymer-assisted assembly of molecular dopants. *Nat. Commun.*, 9, 3956, 2018.
- [13] M. Kruskopf, A. F. Rigosi, A. R. Panna, M. Marzano, D. K. Patel, H. Jin, D. B. Newell, and R. E. Elmquist. Two-Terminal and Multi-Terminal Designs for Next-Generation Quantized Hall Resistance Standards: Contact Material and Geometry. *IEEE Trans. Electron Dev.*, 66, 3973, 2019.
- [14] T. Oe, A. F. Rigosi, M. Kruskopf, B.-Y. Wu, H.-Y. Lee, Y. Yang, R. E. Elmquist, N.-H. Kaneko, D. G. Jarrett. Comparison between NIST Graphene and AIST GaAs Quantized Hall Devices. *IEEE Trans. Instrum. Meas.*, 2019 10.1109/TIM.2019.2930436.
- [15] Schurr J, Ahlers F, Kibble BP. The ac quantum Hall resistance as an electrical impedance standard and its role in the SI. *Measurement Science and Technology*. 2012 Nov 19;23(12):124009.
- [16] Lartsev A, Lara-Avila S, Danilov A, Kubatkin S, Tzalenchuk A, Yakimova R. A prototype of RK/200 quantum Hall array resistance standard on epitaxial graphene. *Journal of Applied Physics*. 2015 Jul 28;118(4):044506
- [17] M. Kruskopf, A. F. Rigosi, A. R. Panna, M. Marzano, D. K. Patel, H. Jin, D. B. Newell, and R. E. Elmquist. Next-generation crossover-free quantum Hall arrays with superconducting interconnections. *Metrologia*, 56, 065002, 2019.
- [18] Novikov S, Lebedeva N, Hämäläinen J, Iisakka I, Immonen P, Manninen AJ, Satrapinski A. Mini array of quantum Hall devices based on epitaxial graphene. *Journal of Applied Physics*. 2016 May 7;119(17):174504.
- [19] Oe T, Gorwadkar S, Itatani T, Kaneko NH. Development of $1/\Omega$ Quantum Hall Array Resistance Standards. *IEEE Transactions on Instrumentation and Measurement*. 2016 Nov 16;66(6):1475-81.
- [20] Woszczyna M, Friedemann M, Dziomba T, Weimann T, Ahlers FJ. Graphene pn junction arrays as quantum-Hall resistance standards. *Applied Physics Letters*. 2011 Jul 11;99(2):022112.
- [21] Park J, Kim WS, Chae DH. Realization of $5 h e 2$ with graphene quantum Hall resistance array. *Applied Physics Letters*. 2020 Mar 2;116(9):093102.
- [22] Hu J, Rigosi AF, Kruskopf M, Yang Y, Wu BY, Tian J, Panna AR, Lee HY, Payagala SU, Jones GR, Kraft ME. Towards epitaxial graphene pn junctions as electrically programmable quantum resistance standards. *Scientific reports*. 2018 Oct 9;8(1):1-1.
- [23] Oe T *et al.* *Conference on Precision Electromagnetic Measurements (CPEM 2020)* 2020 Aug 24 (pp. 1-2). IEEE.
- [24] M. Marzano, M. Kruskopf, A. R. Panna, A. F. Rigosi, D. K. Patel, *et al.* Implementation of a graphene quantum Hall Kelvin bridge-on-a-chip for resistance calibrations. *Metrologia*, 57, 015007, 2020.
- [25] M. Kruskopf, D. M. Pakdehi, K. Pierz, S. Wunderack, R. Stosch, T. Dziomba, M. Götz, J. Baringhaus, J. Aprojanz, C. Tegenkamp, J. Lidzba, T. Seyller, F. Hohls, F. J. Ahlers and H.W. Schumacher Comeback of epitaxial graphene for electronics: large-area growth of bilayer-free graphene on SiC. *2D Mater.*, 3, 041002, 2016.
- [26] Y. Yang, L.-I. Huang, Y. Fukuyama, F.-H. Liu, M. A. Real, P. Barbara, C.-T. Liang, D. B. Newell, and R. E. Elmquist, Low Carrier Density Epitaxial Graphene Devices on SiC. *Small*, 11, 1, 90 – 95, 2015.
- [27] A. F. Rigosi, C.-I. Liu, N. R. Glavin, Y. Yang, H. M. Hill, J. Hu, A. R. Hight Walker, C. A. Richter, R. E. Elmquist, and D. B. Newell, Electrical Stabilization of Surface Resistivity in Epitaxial Graphene

Systems by Amorphous Boron Nitride Encapsulation. *ACS Omega*, 2, 2326–2332, 2017.

- [28] Götz M, Drung D, Pesel E, Barthelmess H-J, Hinrichs C, Afmann C, Peters M, Scherer H, Schumacher B and Schurig Th 2009 Improved cryogenic current comparator setup with digital current sources *IEEE Trans. Instrum. Meas.* 58 1176–82.
- [29] Drung D and Storm J H 2011 Ultralow-noise chopper amplifier with low input charge injection *IEEE Trans. Instrum. Meas.* 60 2347–52.
- [30] B. Jeckelmann and B. Jeanneret, *Rep. Prog. Phys.* 64, 1603 (2001).
- [31] Delahaye F, Jeckelmann B. Revised technical guidelines for reliable dc measurements of the quantized Hall resistance. *Metrologia*. 2003 Sep 2;40(5):217.



Shamith U. Payagala received the B.S. degree in electrical engineering from the University of Maryland, College Park, MD, in 2015, and the M.S. degree in electrical engineering from Johns Hopkins University, Baltimore in 2019. In 2014, he joined the National Institute of Standards and Technology (NIST) as a guest researcher from the University of

Maryland. During this time, he worked in the DC high resistance area on the automation of resistance calibration systems. In 2015, he joined NIST full time as an electrical engineer working on improving resistance bridges, standards, & low current techniques in the NIST Metrology of the Ohm Project.



Albert F. Rigosi (M'17) was born in New York, NY, USA in 1989. He received the B.A., M.A., M.Phil., and Ph.D. degrees in physics from Columbia University, New York, NY, in 2011, 2013, 2014, and 2016, respectively.

From 2008 to 2015, he was a Research Assistant with the Columbia Nano Initiative. From 2015 to 2016, he was a Joint Visiting Research Scholar with the Department of Applied Physics of Stanford University in Stanford, CA, and the PULSE Institute of SLAC National Accelerator Laboratory in Menlo Park, CA. Since 2016, he has been a Physicist at the National Institute of Standards and Technology in Gaithersburg, MD. His research interests include two-dimensional electron systems and applications of those systems' behaviors for electrical metrology.

Dr. Rigosi is a member of the American Physical Society and the Mellon-Mays Initiative of The Andrew W. Mellon Foundation. He was awarded associateships and fellowships from the National Research Council (USA), the Optical Society of America, the Ford Foundation, and the National Science Foundation (Graduate Research Fellowship Program).



Alireza R. Panna was born in Mumbai, India. He received the B.S. degree in electrical engineering from the University of Maryland, College Park, MD, in 2013.

From 2012 to 2013 he worked as a guest researcher for the National Institute of Standards and Technology (NIST),

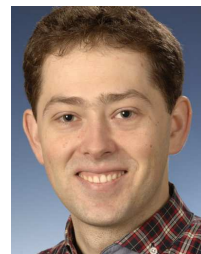
Gaithersburg, MD, where he was involved in magnet characterization for the NIST-4 watt balance. From 2013 to 2017 he was with the National Institutes of Health, Bethesda, MD, where he worked on controls and characterization of various x-ray imaging modalities.

He is currently with the National Institute of Standards and Technology where he is involved in the Metrology of the Ohm and the Quantum Conductance Projects.



Alessio Pollarolo was born in Acqui Terme, Italy, on September 18, 1979. He received the M.S. degree in electronic engineering and the Ph.D. degree in metrology from Politecnico di Torino, Torino, Italy, in 2007 and 2011, respectively. From March 2006 to June 2009, he was with the Electromagnetic Division, Istituto Nazionale di Ricerca

Metrologica (INRiM), Torino, where he worked in Johnson noise thermometry. Since July 2009, he has been with the National Institute of Standards and Technology, Boulder, CO, USA, as a Guest Researcher and is working on the Johnson noise thermometry program.



Mattias Kruskopf was born in Hamburg, Germany, in 1984. He received the M.Sc. degree in electronics engineering, with the focus on metrology, from the Bremen University of Applied Sciences, Bremen, Germany, in 2013. In 2017, he finished his Ph.D. research on epitaxial graphene for quantum resistance metrology in the working group of Low-dimensional

Electron Systems at the Physikalisch-Technische Bundesanstalt (PTB), Braunschweig, Germany.

At the National Institute of Standards and Technology (NIST), Gaithersburg, MD, he focused on improving the scalability and the adoption of graphene-based resistance standards. He has since returned to the Physikalisch-Technische Bundesanstalt (PTB), Braunschweig, Germany.



Stephan Schlamminger (M'12) was born in Kelheim, Germany. He received the Diploma degree in physics from the University of Regensburg, Regensburg, Germany, in 1998, and the Ph.D. degree in experimental physics from the University of Zürich, Zürich, Switzerland, in 2002.

He was with the University of Washington, Seattle, WA, USA, where he was involved in the experimental test of the equivalence principle, from 2002 to 2010. He is currently with the National Institute of Standards and Technology (NIST), Gaithersburg, MD, USA, where he is involved in the watt balances NIST-3 and NIST-4.



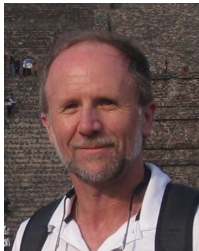
Dean G. Jarrett was (S'88–M'90–SM'99) was born in Baltimore, MD, in 1967. He received the B.S. degree in electrical engineering from the University of Maryland, College Park, in 1990 and the M.S. degrees in electrical engineering and applied biomedical engineering from Johns Hopkins University, Baltimore, in 1995 and 2008, respectively.

Since 1986, he has been with the National Institute of Standards and Technology (NIST), in Gaithersburg, MD, where he was a Cooperative Education Student from the University of Maryland. During this time, he worked in the DC resistance area on the automation of resistance calibration systems. In 1991 he joined NIST full time as an electrical engineer working on the development of an automated AC resistance calibration system and the development of new resistance standards. Since 1994, he has worked in the high resistance laboratory developing automated measurement systems and improved standard resistors to support high resistance calibration services and key comparisons. Since 2014, he has led the Metrology of the Ohm Project at NIST.



Ryan Brown was born in Brockville, Ontario, Canada on January 24th, 1979. He received his diploma in Electronics Engineering in 2002. He has been with Measurements International since 2002 with Primary research focused on DC Resistance and the Quantum Hall Effect (QHE). Since 2002, he has installed over 20 QHE systems

throughout the world to various National Metrology Institutes and Primary Level Laboratories.



Randolph E. Elmquist (M'90–SM'98) received the Ph.D. degree in physics from the University of Virginia, Charlottesville, VA, in 1986. He leads the Quantum Conductance project at the NIST. Working for the past 32 years in the field of electrical and quantum metrology, he has contributed to the experimental design and measurement of

the electronic Kilogram and calculable impedance standards for the determination of the von Klitzing constant and alpha, the unitless fine structure constant. He leads the development of cryogenic current comparator systems, the quantum Hall effect, and graphene electronic devices for metrology.

Dr. Elmquist is a member of the American Physical Society.



Duane Brown was born in Soperton, Ontario, Canada on December 8th, 1948. He worked for Guildline Instruments from 1973 – 1987 in the production and engineering departments. His focus was to support the DC Current Comparator

Development and Technology with the 9975 Manual Resistance Bridge. In 1987 Duane founded Measurements International. Since then Duane has contributed multiple commercial products to the field of Electrical Metrology with the most noticeable being the 6010 DC Resistance Bridge. In 2012 Duane was awarded the NCSLI Wildhack Award for outstanding contribution to the field of Metrology.



David B. Newell received his B.S. in physics and B.A. in mathematics from the University of Washington, Seattle and his Ph. D. in physics from the University of Colorado.

He was awarded the NRC postdoctoral fellowship to work on the Watt Balance Project at the National Institute of Standards and Technology (NIST) in Gaithersburg, MD, and became a full-time staff member in 1996. He has worked on measurements for realizing micro- and nano-scale forces traceable to the SI, was leader the Fundamental Electrical Measurements (FEM) group from 2004 to 2010, helped establish the use of graphene in quantum electrical standards, worked with a NIST team to construct a new watt balance to realize the kilogram from a fixed value of the Planck constant, and, as chair of the CODATA Task Group on Fundamental Constants, provided the exact values of the fundamental constants to be used in the new SI.

He has presently again accepted responsibility as leader of the FEM group. He is a member of the Philosophical Society of Washington, chair for the CODATA Task Group on Fundamental constants, and Fellow of the American Physical Society.